

 Open access • Journal Article • DOI:10.1109/TMTT.2009.2022809

## Long Wavelength VCSEL-by-VCSEL Optical Injection Locking — [Source link](#)





A. Hayat, [Alexandre Bacou](#), [Angélique Rissons](#), [Jean-Claude Mollier](#) ...+3 more authors

**Published on:** 05 Jun 2009 - [IEEE Transactions on Microwave Theory and Techniques](#) (Institute of Electrical and Electronics Engineers)

**Topics:** [Injection locking](#), [Cutoff frequency](#), [Vertical-cavity surface-emitting laser](#), [Optical polarization](#) and [Optical amplifier](#)

Related papers:

- [Injection locking of VCSELs](#)
- [Voltage Spectroscopy and the Operating State of an Optically Injected Long Wavelength VCSEL](#)
- [107-GHz Resonance Frequency of 1.55- \$\mu\$ m VCSELs under ultra-high optical injection locking](#)
- [Light-Induced Transverse-Mode Switching of a Vertical-Cavity Surface-Emitting Laser For Optical Signal Processing](#)
- [Precise frequency stabilization technique for 850nm vertical cavity surface emitting lasers by controlling their optical beat frequency](#)

Share this paper:    

View more about this paper here: <https://typeset.io/papers/long-wavelength-vcSEL-by-vcSEL-optical-injection-locking-4zsotm44vj>



## Open Archive Toulouse Archive Ouverte (OATAO)

OATAO is an open access repository that collects the work of Toulouse researchers and makes it freely available over the web where possible.

This is an author-deposited version published in: <http://oatao.univ-toulouse.fr/>  
Eprints ID: 2193

To link to this article: DOI: 10.1109/TMTT.2009.2022809

URL:<http://ieeexplore.ieee.org/search/wrapper.jsp?arnumber=50669>  
90

**To cite this version:** BACOU, Alexandre. HAYAT, Ahmad. IAKOVLEV, Vladimir. KAPON, Eli. MOLLIER, Jean-Claude. RISSONS, Angélique. SIRBU, Alexei. Long wavelength VCSEL-by-VCSEL optical injection-Locking. *IEEE transactions on microwave theory and techniques*, 2009, vol. 57, n°7, pp. 1850-1858, ISSN 0018-9480

Any correspondence concerning this service should be sent to the repository administrator:  
[staff-oatao@inp-toulouse.fr](mailto:staff-oatao@inp-toulouse.fr)

# Long Wavelength VCSEL-by-VCSEL Optical Injection-Locking

Ahmad Hayat, *Student Member, IEEE*, Alexandre Bacou, *Member, IEEE*, Angélique Rissons, Jean-Claude Mollier, *Member, IEEE*, Vladimir Iakovlev, Alexei Sirbu, *Senior Member, IEEE* and Eli Kapon, *Fellow, IEEE*

**Abstract**—VCSEL-by-VCSEL optical injection-locking to obtain high cut-off frequencies of 1.3  $\mu\text{m}$  Vertical-Cavity Surface-Emitting Lasers (VCSELs) is demonstrated. A detailed physical explanation of the underlying mechanism is presented. VCSELs from the same wafer have been used in a master-follower configuration. Two probe stations are used in this experiment to power-up two VCSELs simultaneously. Polarization insensibility of the injection-locking is demonstrated and a novel architecture is proposed to achieve cut-off frequency doubling. For the first time a high cut-off frequency is achieved through optically injection-locking the satellite mode of a long wavelength VCSEL. Injection-locking spectra with variable injection-powers and variable detuning values have been obtained and methods have been proposed to obtain high cut-off and/or resonance frequencies. A rate-equation based model is presented. Simulations have been carried out using this model. Finally, a linear increase in the follower VCSEL cut-off frequency with increasing injected-power is demonstrated by using a semiconductor optical amplifier.

**Index Terms**—1.3  $\mu\text{m}$  VCSEL, Optical Injection-Locking, Probe Station Testing, Microwave Response of VCSELs

## I. INTRODUCTION

SEMICONDUCTOR lasers are integral components of telecommunication and data communication systems. Their deployment in high-speed telecom and datacom links requires the utilization of external modulators. This is done in order to address two main performance issues related to semiconductor optical sources namely the frequency-chirping under direct modulation and the intrinsic modulation frequency limits imposed by the device structure. The employment of external modulators however renders the system expensive.

Optical injection-locking can be used to overcome these intrinsic limitations of semiconductor lasers. Adler first studied the locking phenomenon in electronic oscillators in 1946 [1]. Pantell then extended the concept of injection-locking of oscillators to optical injection-locking of laser oscillators in 1965 [2]. Optical injection-locking was then demonstrated for He-Ne lasers [3], for CO<sub>2</sub> lasers [4] and for semiconductor lasers [5] over the following two decades. Several optical injection-locking studies regarding

semiconductor lasers have reported frequency-chirp reduction [6], [7], [8], increased RF link gain [8], [9], improved relative intensity noise [10], [11], [12], [13] and diminished non-linear distortion [8], [14]. Despite all these advances regarding this very potent combination of semiconductor lasers and optical injection-locking, the phenomenon and its practical applications could not get any commercial breakthrough. In our opinion, the major reason was the non-integrability of the optical injection-locking laboratory experimental setup into a single chip or even a single module. External modulators continue to be used despite all the improvements demonstrated by the utilization of optical injection-locking. Simply because they are the most cost-effective solution providing the required performance.

With the arrival of Vertical-Cavity Surface-Emitting Lasers (VCSELs) on the commercial scene as low-cost, integrable sources, the efforts to revive the optical injection-locking phenomena were once again undertaken and follower VCSEL resonance frequencies ranging from 27 GHz to 107 GHz have been reported in recent years [8], [15], [16], [17]. The problem of non-integrability however is still unresolved due to the utilization of a distributed feedback (DFB) laser as master optical source to injection-lock a follower VCSEL. The DFB lasers have horizontal optical cavities. This physical asymmetry renders the monolithic integration more complicated while the utilization of a powerful DFB laser compromises the economy of the setup by increasing the cost dramatically and fails the purpose of using a VCSEL in the first place. Clearly the solution to afore-mentioned problems would be to try a VCSEL-by-VCSEL optical injection-locking approach.

We present here, for the first time, a complete study of the microwave behavior of a VCSEL-by-VCSEL optically injection-locked system. Our objective is to explore the possibilities of VCSEL-by-VCSEL optical injection-locking with the final intent to have an integrated low-cost high-speed communications module. In place of working with a master DFB laser and a follower VCSEL, we have decided to work with two identical VCSELs used in the familiar master-follower configuration. In this paper we present the modified rate equations quantifying the follower VCSEL behavior under external light injection. A novel architecture using a 50-50 coupler is proposed along with the familiar optical circulator architecture. We then present the several experimental results obtained through working in different detuning and

A. Hayat, A. Bacou, A. Rissons and J-C. Mollier are with DEOS, Institut Supérieur de l'Aéronautique et de l'Espace (ISAE), Université de Toulouse, Toulouse 31055, France (e-mail: ahmad.hayat@isae.fr).

V. Iakovlev is with BeamExpress S.A., Lausanne 1015, Switzerland. A. Sirbu is with Laboratory of Physics of Nanostructures, Ecole Polytechnique Fédérale de Lausanne (EPFL). E. Kapon is with both BeamExpress and the Laboratory of Physics of Nanostructures, EPFL.

injection regimes. A comprehensive physical explanation to interpret the results thus obtained is also given. Finally damped frequency responses of an injection-locked follower VCSEL are presented for various increasing injected-power levels to demonstrate the effective bandwidth enhancement of the system through proper choice of the detuning mechanism.

## II. THEORY AND PHYSICAL EXPLANATION

The increase in resonance frequency is a combination of two factors extraneous to the follower laser and dependent on the injected light.

- 1) The injection of photons in the follower laser cavity changes the carrier-photon equilibrium inside the cavity. The free-running follower laser cavity resonance that is represented by the photon and carrier densities is redefined due to external light injection. The increase in photon density affects the carrier density inside the follower laser cavity. The change in cavity resonance frequency due to carrier population density variation can be quantified using “ $\alpha_H$ ”; the linewidth enhancement factor that indicates the carrier-variation induced refractive index change and hence the amplitude-phase coupling.

The consequence of the external photon-injection is hence a downshift in the laser cavity resonance frequency denoted as  $\omega_{Downshifted}$  in this text.

- 2) The second factor takes into account the difference between the master and the follower lasing frequencies. This difference is known as “frequency detuning” and could be defined as

$$\Delta\omega = \omega_{master} - \omega_{follower} \quad (1)$$

The detuning is said to be positive if the master laser has an emission frequency greater than that of the follower laser and is said to be negative if the reverse is true. Once locked the follower laser emits at the same frequency as the master laser. The output frequency of the follower laser hence becomes identical to that of the master laser.

The follower laser, therefore, in effect is experiencing two different phenomena at the same time. The external light injection has offset the cavity mode to a lower resonance frequency while the detuning has led to a high emission frequency. It is the difference between  $\omega_{master}$  and  $\omega_{Downshifted}$  that determines the value of enhanced resonance frequency,  $\omega_{EnhancedResonance}$  of an optically injection-locked laser. The interference between  $\omega_{master}$  and  $\omega_{Downshifted}$  generates a beat note whose value could be given as

$$\omega_{EnhancedResonance} = \omega_{master} - \omega_{Downshifted} \quad (2)$$

The resonance peak observed in  $S_{21}$  curves of an optically injection-locked slave laser is in fact the beat-note between the downshifted cavity resonance frequency,  $\omega_{Downshifted}$ , and the master laser emission frequency  $\omega_{master}$ . This beat-note is amplified due to resonance when the modulating frequency

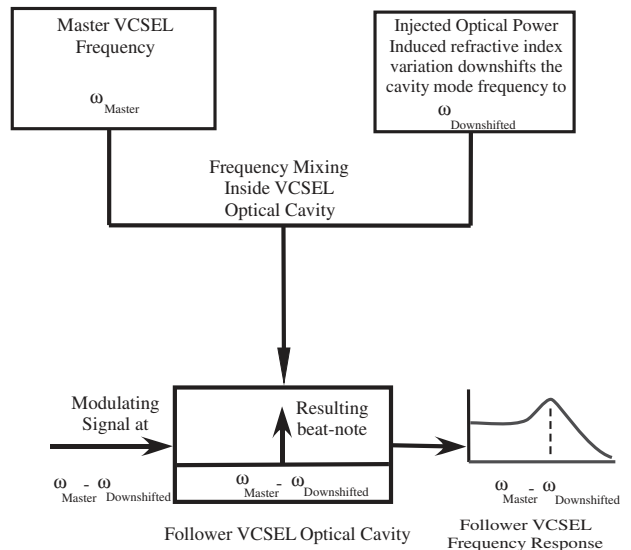


Fig. 1. A schematic diagram representing the physical phenomenon of resonance frequency enhancement of the follower VCSEL due to optical injection-locking. The beat note  $\omega_{master} - \omega_{Downshifted}$  created due to frequency-mixing inside the follower VCSEL optical cavity is amplified due to resonance when a signal with a same frequency value is applied to modulate the follower VCSEL.

becomes equal to it. Fig. 1 represents the physical phenomena taking place during the optical injection-locking procedure schematically.

(2) explains the high resonance frequencies for optically injection-locked follower lasers operating in positive frequency detuning regime. A positive frequency detuning value leads to a high resonance frequency. These high resonance frequencies, obtained through operating in positive frequency detuning regimes, however, do not help in increasing the overall 3-dB bandwidth of the system because the resonance is pronounced so far on the frequency spectrum that the  $S_{21}$  curve has already tapered down to below 3-dB of the DC gain [16].

When the follower laser is injection-locked in the negative frequency detuning operation regime, quite logically the enhancement in the optically injection-locked follower laser frequency is not colossal. However, this resonance, by virtue of not being very high in frequency, falls within the operating limits of the lasing device and increases the overall bandwidth of the system along with the DC gain. Furthermore Murakami et al. [18] have shown that the carrier population density induced variation in the cavity resonance can be mathematically described as follows:

$$\omega_{Shifted} = \frac{\alpha_H}{2} \cdot a_0 \cdot \Delta N \quad (3)$$

where  $a_0$  represents the differential gain and  $\Delta N$  is the variation in the carrier population density.

(3) shows that the value of  $\omega_{Shifted}$  depends on  $\Delta N$ . Since this variation is affected by injecting optical power from the master laser inside the follower laser cavity, varying the injected power varies the cavity resonance frequency of the optically injection-locked laser. An increase in photon population

inside the follower laser cavity through optical injection downshifts the cavity resonance frequency and (ref. (2) and (3)) increases the  $\omega_{EnhancedResonance}$ . The  $\omega_{EnhancedResonance}$  therefore is directly proportional to the injected optical power. Numerous authors have already presented  $S_{21}$  curves of optically injection-locked follower lasers to demonstrate this effect [8], [17], [15].

### III. DEVICE CHARACTERISTICS

The VCSELs used in this experiment are double intracavity contact 1.3  $\mu\text{m}$  single-mode VCSELs with coplanar access. The InP-based optical cavity consists of four InAlGaAs quantum wells (ref. Fig. 2). The top and bottom distributed Bragg reflectors (DBRs) comprise of 21 and 35 pairs respectively and are grown by metal-organic chemical vapor deposition (MOCVD) epitaxy method. Using the technique of localized wafer fusion, the top and the bottom AlGaAs-GaAs DBRs are then bonded to the active cavity wafer and the tunnel junction mesa structures [19], [20]. Using VCSELs with double intracavity contacts has its own advantages. These contacts are much nearer to the active region than the classical contacts. Their utilization combined with the presence of tunnel junction allows to have lower series resistance as compared to oxidized-aperture VCSELs. Due to this proximity to the active region these VCSELs tend to have a high quantum efficiency. The devices used in this experiment have an average threshold of 1mA. Their location near the active region results in no current passage through DBRs.

For this series of experiments, we have decided to use un-packaged, un-cooled, on-chip VCSELs. This method is advantageous in certain regards. It provides direct electrical-access to the VCSEL optical cavity and the device performance is not curtailed by package-induced parasitics. VCSELs from the same wafer have been used to investigate the possibility of VCSEL-by-VCSEL optical injection-locking. That helps avoid using the polarization maintaining techniques that are necessary to use in case of non-identical master and follower lasers.

Another problem that surfaces while working at high frequencies is the introduction of parasitic inductances and capacitances due to device packaging. The high frequency performance of the component is affected by these parasitics since at high frequencies the reactance values for the capacitors and inductors are non longer negligible. At high frequencies, instead of reaching the VCSEL optical cavity, the incoming signal is routed through the parasitic components. This undesired bypassing effect severely degrades the output of the component. In most cases, the component cut-off frequency is dictated by the packaging parasitic cut-off bandwidth. Post-experimental treatment of the data thus acquired is necessary to extract useful information [8], [15], [21]. Using on-chip components eliminates the packaging and hence the parasitics effects associated to it. In order to obtain the true VCSEL optical cavity small-signal response under

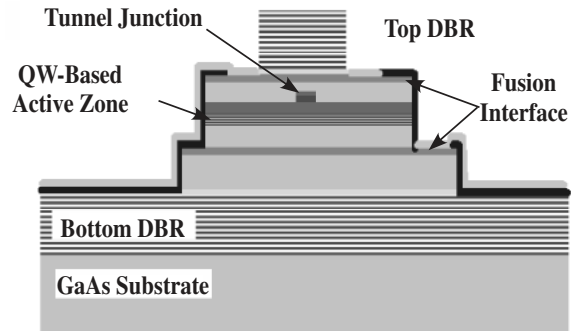


Fig. 2. Schematic of the 1.3  $\mu\text{m}$  structure used in optical injection-locking experiments.

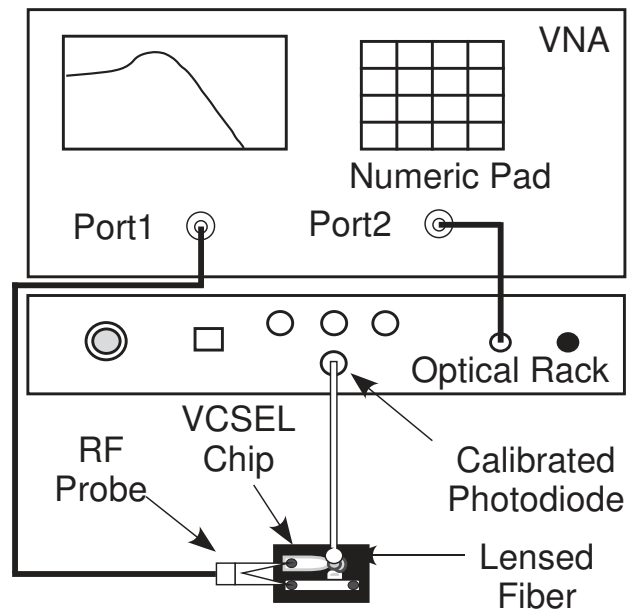


Fig. 3. Schematic representation of the experimental setup used to measure the  $S_{21}$  response of an on-chip VCSEL using a vector network analyzer. A lensed fiber is used to collect the optical power emitted by the VCSEL. The VCSEL optical output is converted to electrical signal by a pre-calibrated photodiode integrated to the vector network analyzer by means of an optical rack.

external light injection it was decided to use on-chip VCSELs.

On the other hand, coupling optical power from the small emission window of a VCSEL to a lensed single-mode fiber becomes challenging at times due to low optical power emission levels of the VCSELs and due to the miniscule nature of the components deployed in this experiment. In our opinion however, the results thus obtained justify the extra effort employed.

### IV. MEASUREMENTS

#### A. Working Environment

In order to power-up the VCSELs, probe stations have been used. Since the intent of the experiments has been to investigate the VCSEL-by-VCSEL optical injection-locking



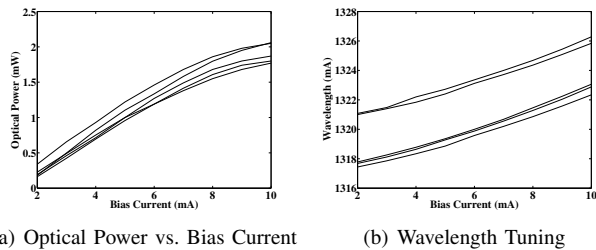


Fig. 4. The L-I curves for the set of VCSELs used in this experiment. Representative wavelength-bias current tuning curves are also given.

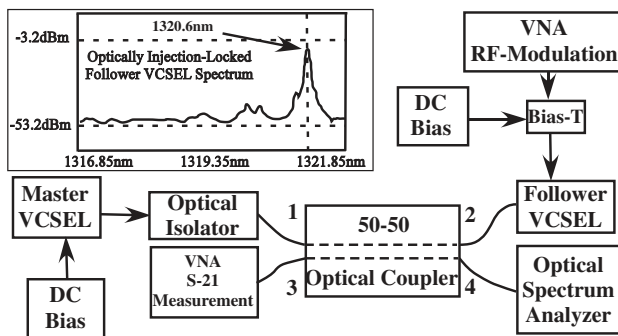


Fig. 5. The proposed architecture employing a 4-port optical coupler for injection-locking experiments.

phenomenon, two probe stations have been used simultaneously to power-up the master and the follower lasers at a time. Furthermore, the follower VCSEL probe station has been connected to an HP-8510 Vector Network Analyzer (VNA). This VNA has been used to serve two purposes.

- 1) To provide modulation signal to the optically injection-locked follower VCSEL.
- 2) To observe the  $S_{21}$  response of the optically injection-locked follower VCSEL under external light injection.

An optical rack has been integrated to the VNA. This rack consists of a high-speed photodiode calibrated to the VNA. The probes were calibrated using the VNA before the experiment to obtain the parasitics-free VCSEL optical-cavity small-signal response. On the output side of the injection-locked system, the light emitted from the follower VCSEL was gathered using an unsheathed lensed single-mode fiber. This fiber was then connected to the optical rack containing the photodiode already calibrated to the VNA. A schematic representation of the experimental setup used to measure the on-chip VCSELs'  $S_{21}$  response is presented in Fig. 3.

No temperature regulation or compensation mechanism was employed in course of this experiment and all the experiments were carried out at room temperature. The output optical powers and the emission spectra of the VCSELs utilized in this experiment are given in Fig. 4.

### B. Architectures Used for Injection-Locking Experiments

The standard architecture used for injection-locking experiments is a polarization-maintaining circulator. In our opinion the utilization of polarization-maintaining

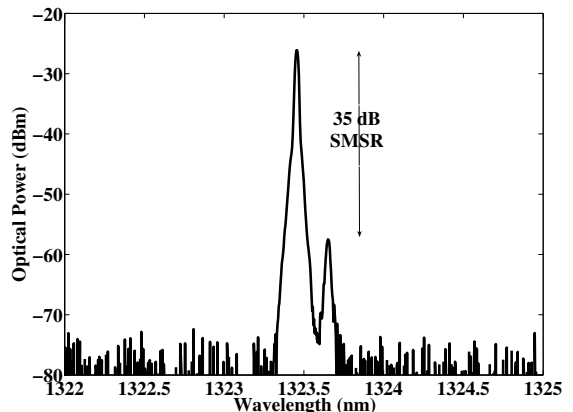


Fig. 6. Optical spectrum of the follower VCSEL used in the injection-locking experiment utilizing the 4-port coupler. A smaller secondary mode could also be observed to the right of the fundamental lasing mode. The side-mode suppression ratio (SMSR) is noted to be about 35 dBs.

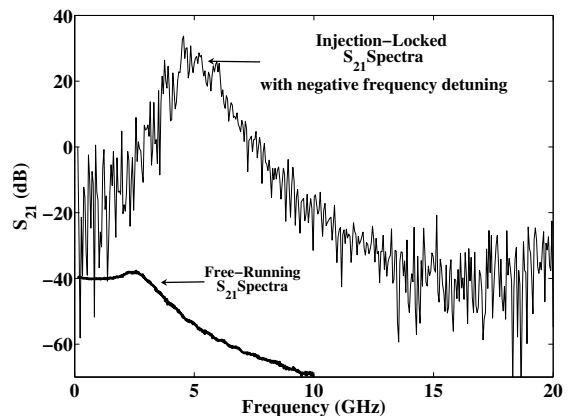


Fig. 7. A comparison of the  $S_{21}$  spectra of free-running and optically injection-locked  $1.3 \mu\text{m}$  single-mode VCSELs. The follower VCSEL was locked using the architecture shown in Fig. 5. The measurements were taken in the negative frequency detuning regime.

circulator was rendered necessary due to the fact that two fundamentally different laser sources with inherently different polarizations, namely a DFB laser and a VCSEL, were being used in these experiments [8], [15], [22]. We decided to use a non-polarization maintaining 3-dB 4-port coupler to investigate this hypothesis. A schematic representation of the experimental setup is presented in Fig. 5. The fundamental supporting argument was that the choice of two identical VCSELs functioning at approximately same bias currents would have the same polarization. The follower VCSEL optical spectrum is given in Fig. 6. The side-mode suppression ratio between the fundamental and the satellite mode is about 40 dBs. We decided to injection-lock the follower VCSEL satellite mode with master VCSEL fundamental mode since we had decided not to use the semiconductor optical amplifier. This technique hitherto had been limited to optical computing applications [23]. The results thus obtained are given in Fig. 7.

In order to investigate the variation in optically injection-

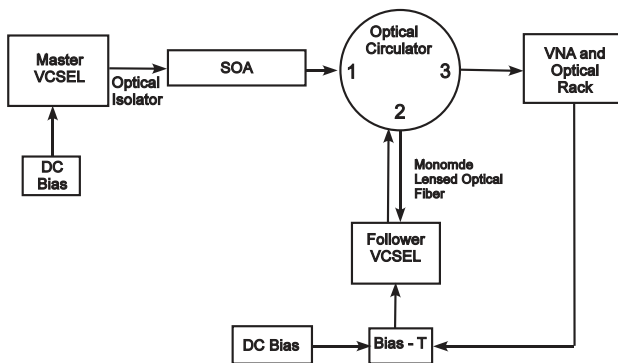


Fig. 8. Experimental Setup. The  $1.3 \mu\text{m}$  follower VCSEL was optically injection locked using a 3-port optical circulator. A semiconductor optical amplifier (SOA) was used to vary the incident power levels. The  $S_{21}$  response of the injection-locked VCSEL was observed using an HP-8510C vector network analyzer (VNA).

locked follower VCSEL dynamic response ( $S_{21}$ ) with variation in injected-power levels and detuning, a semiconductor optical amplifier in combination with a polarization-maintaining optical circulator was used. Using an semiconductor optical amplifier gives the freedom of varying the injected optical power without interfering with the master VCSEL bias current and therefore the master VCSEL emission wavelength. In this way the variations in the follower VCSEL  $S_{21}$  response due to the injected optical power variation and due to the detuning variation can be completely decorrelated and studied independently. A schematic representation of the experimental setup is given in Fig. 8.

## V. RESULTS

Free-running and injection-locked spectra for the follower VCSEL are presented in Fig. 10 when it is injection-locked with a fixed positive frequency detuning (negative wavelength detuning) value. As discussed in II, a positive frequency detuning (negative wavelength detuning) produces a large difference between the cavity mode frequency and the follower VCSEL emission frequency which is in fact locked to the master VCSEL emission frequency. The beat-note generated due to the difference in these two frequencies is amplified due to resonance when a modulating signal at the same frequency as of the beat-note is applied to the injection-locked follower VCSEL. Increasing the injected optical power (ref. Injection-Locked  $S_{21}$  spectra in Fig. 10) only shifts the resonant peak towards higher frequencies by varying the carrier population density dependent cavity refractive index quantified by (2) and (3) without dampening the response. Fig. 9 represents two more curves obtained using positive frequency detuning (negative wavelength detuning). The lower value of the resonant frequency is due to lower injected optical power levels while the somewhat diminished sharpness of the resonant peak is due to a lesser degree of detuning.

On the other hand, Fig. 11 presents the  $S_{21}$  response of an optically injection-locked follower VCSEL with a

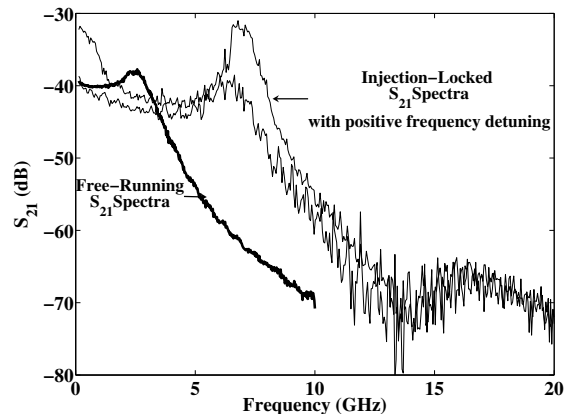


Fig. 9. Small-signal frequency response ( $S_{21}$ ) of free-running and injection-locked VCSEL spectra: The injection-locked spectra were obtained by locking the follower laser at a positive frequency detuning (wavelength detuning of  $-0.04 \text{ nm}$ ). The respected injected optical powers for the two injection-locked spectra are  $9 \text{ dBm}$  and  $10.2 \text{ dBm}$ . An increase in injected optical power shifts the resonant peak toward a higher frequency.

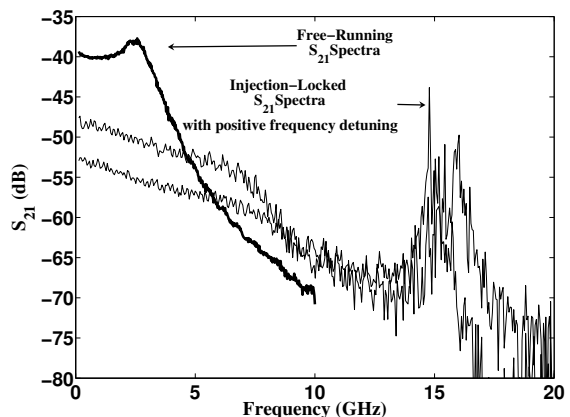


Fig. 10. Small-signal frequency response ( $S_{21}$ ) of free-running and injection-locked VCSEL spectra: The injection-locked spectra were obtained by locking the follower laser at a positive frequency detuning ( a negative wavelength detuning of  $-0.09 \text{ nm}$ ). The respected injected optical powers for the two injection-locked spectra are  $10.8 \text{ dBm}$  and  $12.3 \text{ dBm}$  respectively. These spectra are similar to those shown in Fig. 9 except that the injection power levels and detuning are increased. A four-fold increase in the resonance frequency can be observed.

negative frequency (positive wavelength) detuning. As argued in II, due to negative frequency detuning the resonant peak frequency value is not very big but on the other hand the response is very flat. Compared to Fig. 10 and Fig. 9, the 3-dB bandwidth is increased due to the employment of negative frequency detuning (positive wavelength detuning) improving the overall system bandwidth. Fig. 10 and Fig. 9 improve the resonance frequency value by two-fold and four-fold respectively but fail to improve the 3-dB bandwidth.

Finally Fig. 12 presents several injection-locked  $S_{21}$  spectra for the follower VCSEL. These spectra have been obtained by working in a fixed negative frequency detuning (positive wavelength detuning) regime. Several curves with increasing injection powers and consequently increasing 3-dB bandwidths

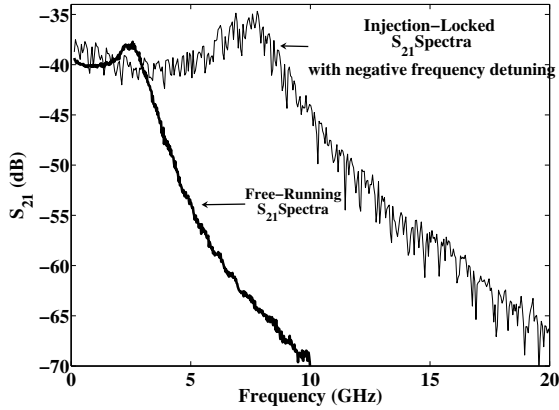


Fig. 11. Small-signal frequency response ( $S_{21}$ ) of free-running and injection-locked VCSEL spectra: The injection-locked spectrum was obtained by locking the follower laser at a negative frequency detuning value (a wavelength detuning +0.101 nm). The injected optical power is 13.9 dBm.

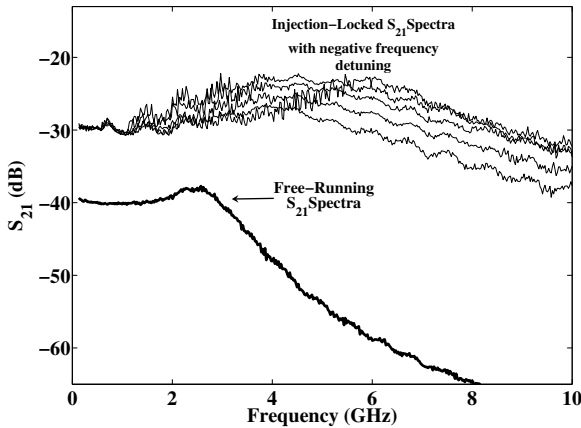


Fig. 12. Small Signal frequency response ( $S_{21}$ ) of a 1.3  $\mu\text{m}$  wafer-fusion single-mode injection-locked VCSEL for different incident optical powers. Corresponding cut-off frequencies are also indicated. The small signal frequency response of the same VCSEL in free-running mode is also presented for comparison.

were obtained. The increase in effective bandwidth is due to increase in photon population density that downshifts the cavity-mode frequency hence increasing the value of  $\omega_{EnhancedResonance}$  (ref. (2)). The high damping of the curves however is due to the selection of negative frequency detuning (positive wavelength detuning of 0.152 nm) regime. The 3-dB bandwidth has shown a two-fold increase for this last set of curves depicted in Fig. 12. Since the frequency detuning for these particular measurements is kept constant, the resonance frequency and hence the cut-off frequency follows the variation in injected optical power. The injected-power levels corresponding to the progressive optically injection-locked follower VCSEL  $S_{21}$  spectra are 6 dBm, 9 dBm, 10.2 dBm, 11.5 dBm and 12.3 dBm respectively. Fig. 13 shows the linear variation of the 3-dB bandwidth with increases injection power levels.

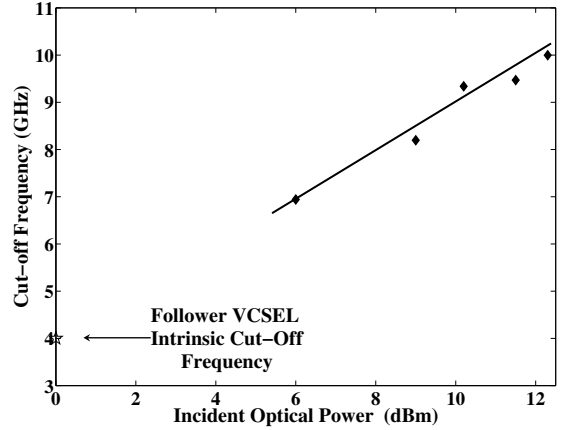


Fig. 13. follower VCSEL intrinsic cut-off frequency as a function of incident optical power. The diamonds represent the measured intrinsic cut-off frequencies under optical injection-locking while the solid line is the data-fitted curve. The follower VCSEL intrinsic cut-off frequency is also presented as reference.

## VI. SIMULATIONS USING RATE EQUATIONS

The optically injection-locked follower VCSEL response is modeled by re-writing the classical rate equations by taking into account the frequency detuning between the two VCSELs, the phase difference thus induced and the optical power coupling rate that determines the effective injected optical power [24]. These modified rate equations are given below. The Langevin forces that typically quantify laser noise in these rate equations have been omitted for simplicity.

$$\frac{dS}{dT} = \frac{\Gamma \cdot v_g \cdot a_0 \cdot (N - N_{tr})S}{1 + \epsilon S} - \frac{S}{\tau_p} + 2\kappa_c \sqrt{S \cdot S_{inj}} \cos(\Delta ft - \phi(t)) + \Gamma B \beta N^2 \quad (4)$$

$$\frac{dN}{dT} = \frac{\eta I}{q \cdot V_{act}} - (A + BN + CN^2) \cdot N - \frac{v_g \cdot a_0 \cdot (N - N_{tr})S}{1 + \epsilon S} \quad (5)$$

$$\frac{d\phi}{dT} = \frac{\alpha_H}{2} \cdot v_g \cdot a_0 \cdot \frac{(N - N_{tr})}{1 + \epsilon S} - \frac{\alpha_H}{2\tau_p} + \kappa_c \sqrt{\frac{S_{inj}}{S}} \cdot \sin(\Delta ft - \phi(t)) \quad (6)$$

Where  $S, N$  and  $\phi$  are photon density, carrier density and the follower laser phase respectively.  $N_{tr}$  is the transparency carrier density.  $\kappa_c$  and  $\beta$  are the optical-coupling and the spontaneous emission coefficients.  $\epsilon, \Gamma$  and  $\alpha_H$  denote the compression, confinement, and amplitude-phase coupling (Henry) factors.  $A, B$  and  $C$  are non-radiative recombination, bimolecular recombination and Auger's recombination rates respectively.  $\tau_p$  is the photon lifetime.  $V_{act}$  is the volume of the active region.  $I$  denotes the bias current.  $S_{inj}$  represents the injected photon density,  $\alpha_o$  the differential gain,  $v_g$  the group velocity and  $\Delta f$  the frequency detuning between the master and the follower lasers. The value for the optical coupling coefficient  $\kappa_c$  has been calculated using the relation



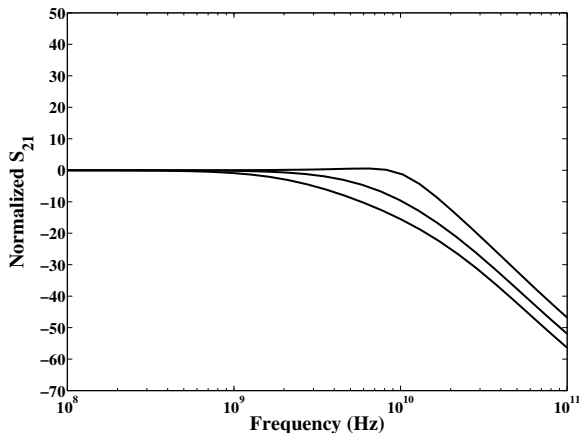


Fig. 14. Optically Injection-Locked follower VCSEL  $S_{21}$  response using the modified rate equations (4,5,6). These highly damped simulation responses have been obtained by keeping a constant injection-ratio and by working on the edge of the negative frequency detuning.

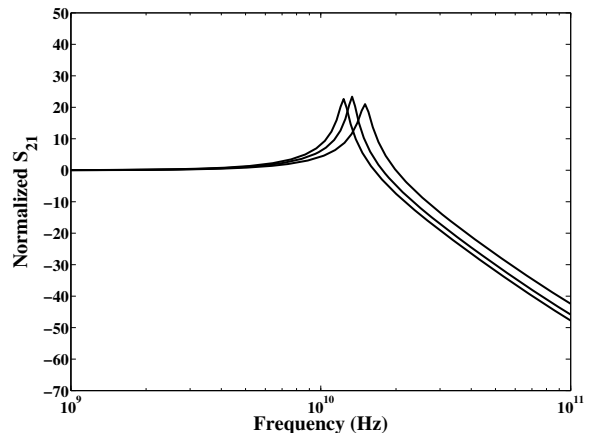


Fig. 15. Optically Injection-Locked follower VCSEL  $S_{21}$  response using the modified rate equations (4,5,6). These under-damped simulation responses have been obtained by keeping a constant injection-ratio and by working on the edge of the positive frequency detuning.

$$\kappa_c = \frac{v_g}{2L_{eff}} \quad (7)$$

where  $L_{eff}$  is the effective cavity length. Since the cavity length for the VCSELs is very small as compared to DFB lasers, the value of coupling coefficient is consequently higher which enables in attaining much higher effective injection-ratios [8].

These equations were solved using MATLAB with the ODESolver45 based on the Rung-Kutta numerical algorithm. The parameters used in the simulations are outlined in Table. I. The simulation curves thus obtained are given in Figs. 14, 15 and 16. Three visibly distinct responses for the optically injection-locked follower VCSEL have been presented. The over-damped, critically-damped and under-damped responses have been obtained by varying the detuning frequency between the master and follower VCSELs.

Fig. 14 gives the  $S_{21}$  responses obtained by working at the negative frequency detuning edge. As a result the  $S_{21}$  responses are highly damped. On the other hand Fig. 15 refers to the  $S_{21}$  responses obtained by doing simulations at the edge of the positive frequency detuning range. These responses are under-damped with sharp resonance frequencies varying from 10 GHz to 20 GHz. The third set of simulations, as depicted in Fig. 16, was obtained by working with small negative detuning frequency values. As a result of the negative frequency detuning values being small, the  $S_{21}$  curves thus obtained are critically-damped.

These simulation results depict the detuning frequency and the injection-ratio dependence of the optically injection-locked follower VCSEL microwave behavior. By varying the detuning-frequency and the injection-ratio properly under-damped, over-damped and critically-damped  $S_{21}$  responses with varying resonance frequencies and hence 3-dB bandwidths can be obtained.

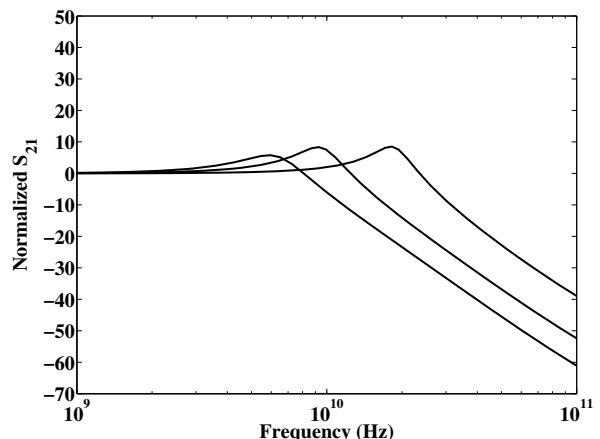


Fig. 16. Optically Injection-Locked follower VCSEL  $S_{21}$  response using the modified rate equations (4,5,6). These critically-damped simulation responses have been obtained by gradually increasing the injection-ratio while working with a slightly negative frequency detuning.

## VII. CONCLUSION

We have reported a thorough study of VCSEL-by-VCSEL optical injection-locking. The intent was to move toward compacter, lighter, low-cost, high-speed systems that could be monolithically fabricated or integrated into communication modules. The injection-locking experiments reported here were carried-out using two probe stations to power-up the master and follower VCSELs. The advantage of such a setup was a parasitics-free  $S_{21}$  response that needed no post-experimental treatment. The injection of optical power in the fibered components however became challenging at times. The back-reflections from the open-ended unsheathed lensed fiber used to collect optical power hinder the obtention of smooth  $S_{21}$  curves. This could be overcome by using anti-reflection (AR) coated conical and ball lensed fibers that gather a maximum of light without perturbing the VCSEL emission.

TABLE I  
VCSEL INTRINSIC PARAMETERS

Parameter	Symbol	Value	Units
Intrinsic Efficiency	$\eta_i$	0.8	-
Carrier Lifetime	$\tau_e$	0.61	ns
Photon Lifetime	$\tau_p$	6.4	ns
Threshold Carrier Density	$N_{th}$	$5.33 \times 10^{18}$	$cm^{-3}$
Transparency Carrier Density	$N_{tr}$	$3.24 \times 10^{18}$	$cm^{-3}$
Non-Radiative Recombination Rate	A	$1.1 \times 10^8$	$s^{-1}$
Bimolecular Recombination Rate	B	$1.0 \times 10^{-10}$	$cm^3/s$
Auger's Recombination Rate	C	$3.6 \times 10^{-29}$	$cm^6/s$
Differential Gain	$a_0$	$4.8 \times 10^{-16}$	$cm^2$
Gain Compression Factor	$\epsilon$	$2.2 \times 10^{-17}$	$cm^3$
Phase-Amplitude Coupling Factor	$\alpha_H$	5	-
Coupling-Rate Coefficient	$\kappa_c$	$1.5 \times 10^{13}$	$s^{-1}$

We have hypothesized that the necessity of employing polarization control and polarization matching in previous injection-locking experiments using VCSELs was due to the dissimilarity between the two optical sources. Ideally, the deployment of two identical VCSELs should result in successful optical injection-locking without polarization control. Results to this effect have been presented in this article since no polarization control mechanism was applied to obtain the  $S_{21}$  curves presented.

The enhancement of effective bandwidth by injection-locking the secondary mode paves the way for the realization of low-cost, high-speed, VCSEL-by-VCSEL, optically injection-locked communication modules. While working with devices, whose intrinsic cut-off limit is about 4 GHz, it has been demonstrated that VCSEL-by-VCSEL injection-locking can be used to have effective bandwidths up to 12 GHz. With the progress of vertical-cavity semiconductor optical amplifier technology [25], [26] combined with the advances in wafer-fusion fabrication techniques, integrated VCSEL-by-VCSEL optically injection-locked modules for high-speed applications seem to be not a distant possibility. Consequently VCSELs could be employed for applications that require direct intensity modulation at high frequencies such as "fiber to the home" (FTTH) or gigabit LAN. The simulations depict that the resonance frequency and the cut-off frequency of an optically injection-locked follower VCSEL can be controlled by varying the injection ratio  $S_{inj}/S$  and the frequency detuning  $\Delta f$ . Increasing injection-ratios tend to enhance the cut-off frequency while the varying frequency detuning can be used to control the damping of the resonance frequency. In this fashion, over-damped, under-damped or critically damped  $S_{21}$  responses can

be obtained.

## REFERENCES

- [1] R. Adler, "A Study of Locking Phenomena in Oscillators," *Proceedings of the IEEE*, vol. 61, no. 10, pp. 1380–1385, Oct. 1973.
- [2] R. Pantell, "The Laser Oscillator With An External Signal," *Proceedings of the IEEE*, vol. 53, no. 5, pp. 474–477, May 1965.
- [3] H. Stover and W. Steier, "Locking of Laser Oscillators by Light Injection," *Applied Physics Letters*, vol. 8(4), p. 91, 1966.
- [4] C. Buczek and R. Freiberg, "Hybrid Injection-Locking of Higher Power  $CO_2$  Lasers," *Quantum Electronics, IEEE Journal of*, vol. 8, No. 7, pp. 641–650, Jul 1972.
- [5] S. Kobayashi and T. Kimura, "Coherence of Injection Phase-Locked AlGaAs Semiconductor Laser," *Electronics Letters*, vol. 16, no. 17, pp. 668–670, 14 1980.
- [6] C. Lin and F. Mengel, "Reduction of Frequency Chirping and Dynamic Linewidth in High-Speed Directly Modulated Semiconductor Lasers by Injection Locking," *Electronics Letters*, vol. 20, no. 25, pp. 1073–1075, 6 1984.
- [7] H. Toba, Y. Kobayashi, K. Yanagimoto, H. Nagai, and M. Nakahara, "Injection-locking Technique Applied to a 170 km Transmission Experiment at 445.8 Mbit/s," *Electronics Letters*, vol. 20, no. 9, pp. 370–371, 26 1984.
- [8] L. Chrostowski, X. Zhao, and C. Chang-Hasnain, "Microwave Performance of Optically Injection-locked VCSELs," *Microwave Theory and Techniques, IEEE Transactions on*, vol. 54, no. 2, pp. 788–796, Feb. 2006.
- [9] H.-K. Sung, T. Jung, D. Tishinin, K. Liou, W. Tsang, and M. Wu, "Optical Injection-Locked Gain-Lever Distributed Bragg Reflector Lasers With Enhanced RF Performance," *Microwave Photonics, 2004. MWP'04. 2004 IEEE International Topical Meeting on*, pp. 225–228, Oct. 2004.
- [10] L. Chrostowski, C.-H. Chang, and C. Chang-Hasnain, "Reduction of Relative Intensity Noise and Improvement of Spur-Free Dynamic Range of an Injection-Locked VCSEL," *Lasers and Electro-Optics Society, 2003. LEOS 2003. The 16th Annual Meeting of the IEEE*, vol. 2, pp. 706–707 vol.2, Oct. 2003.
- [11] N. Schunk and K. Petermann, "Noise Analysis of Injection-Locked Semiconductor Injection Lasers," *IEEE Journal of Quantum Electronics*, vol. 22, no. 5, pp. 642–650, May 1986.
- [12] M. Espana-Boquera and A. Puerta-Notario, "Noise Effects in Injection Locked Laser Simulation: Phase Jumps and Associated Spectral Components," *Electronics Letters*, vol. 32, no. 9, pp. 818–819, Apr 1996.
- [13] G. Yabre, H. De Waardt, H. van den Boom, and G.-D. Khoe, "Noise Characteristics of Single-Mode Semiconductor Lasers Under External Light Injection," *Quantum Electronics, IEEE Journal of*, vol. 36, no. 3, pp. 385–393, Mar 2000.
- [14] X. Meng, T. Chau, D. Tong, and M. Wu, "Suppression of Second Harmonic Distortion in Directly Modulated Distributed Feedback Lasers by External Light Injection," *Electronics Letters*, vol. 34, no. 21, pp. 2040–2041, Oct 1998.
- [15] X. Zhao, M. Moewe, L. Chrostowski, C.-H. Chang, R. Shau, M. Ortsiefer, M.-C. Amann, and C. Chang-Hasnain, "28 GHz Optical Injection-Locked 1.55  $\mu m$  VCSELs," *Electronic Letters, IEE*, vol. Vol. 40 No. 8, 15 April 2004.
- [16] L. Chrostowski, F. B., W. Hoffman, M.-C. Amann, S. Wiczorek, and W. Chow, "40 GHz Bandwidth and 64 GHz Resonance Frequency in Injection-Locked 1.55  $\mu m$  VCSELs," *Journal of Selected Topics in Quantum Electronics, IEEE Journal of*, vol. Vol. 13, No. 5, Sep/Oct 2007.
- [17] X. Zhao, E. K. Lau, D. Parekh, H.-K. Sung, W. Hofmann, M. C. Amann, M. C. Wu, and C. J. Chang-Hasnain, "107-GHz Resonance Frequency of 1.55  $\mu m$  VCSELs Under Ultra-high Optical Injection Locking," in *OSA/CLEO*, 2008.
- [18] A. Murakami, K. Kawashima, and K. Atsuki, "Cavity Resonance Shift and Bandwidth Enhancement in Semiconductor Lasers With Strong Light Injection," *Quantum Electronics, IEEE Journal of*, vol. 39, no. 10, pp. 1196–1204, Oct. 2003.
- [19] V. Iakovlev, G. Suruceanu, A. Caliman, A. Mereuta, A. Mircea, C.-A. Berseth, A. Syrbu, A. Rudra, and E. Kapon, "High-Performance Single-Mode VCSELs in the 1310-nm Waveband," *IEEE Photonics Technology Letters*, vol. 17, no. 5, pp. 947–949, May 2005.

- [20] A. Syrbu, V. Iakovlev, G. Suruceanu, A. Caliman, A. Mereuta, A. Mircea, C.-A. Berseth, E. Diechsel, J. Boucart, A. Rudra, and E. Kapon, "VCSELs Emitting in the 1310-nm Waveband for Novel Optical Communication Applications," *Vertical-Cavity Surface-Emitting Lasers IX*, vol. 5737, no. 1, pp. 167–173, 2005.
- [21] L. Chrostowski, X. Zhao, C. Chang-Hasnain, R. Shau, M. Ortsiefer, and M.-C. Amann, "Very High Resonance Frequency (>40 GHz) Optical Injection-Locked 1.55  $\mu\text{m}$  VCSELs," in *Microwave Photonics. MWP'04. IEEE International Topical Meeting on*, 4-6 Oct. 2004, pp. 255 – 258.
- [22] L. Chrostowski, C.-H. Chang, and C. Chang-Hasnain, "Enhancement of Dynamic Range in 1.55  $\mu\text{m}$  VCSELs Using Injection Locking," *IEEE Photonics Technology Letters*, vol. 15, no. 4, pp. 498–500, April 2003.
- [23] Y. Onishi, N. Nishiyama, C. Caneau, F. Koyama, and C. en Zah, "Dynamic behavior of an all-optical inverter using transverse-mode switching in 1.55  $\mu\text{m}$  vertical-cavity surface-emitting lasers," *Photonics Technology Letters, IEEE*, vol. 16, no. 5, pp. 1236–1238, May 2004.
- [24] —, "All-optical Inverter Based on Long-Wavelength Vertical-Cavity Surface-Emitting Laser," *Selected Topics in Quantum Electronics, IEEE Journal of*, vol. 11, no. 5, pp. 999–1005, Sept.-Oct. 2005.
- [25] G. Cole, E. Bjorlin, C. Wang, N. MacDonald, and J. Bowers, "Widely Tunable Bottom-Emitting Vertical Cavity SOAs," *IEEE Photonics Technology Letters*, vol. vol. 17, no. 12, Dec. 2005.
- [26] T. Kimura, S. Bjrlin, J. Piprek, and J. Bowers, "High-Temperature Characteristics and Tunability of Long-Wavelength Vertical-Cavity Semiconductor Optical Amplifiers," *IEEE Photonics Technology Letters*, vol. Vol. 15, No. 11, Nov. 2003.



**Ahmad Hayat** (S'06) was born in Wah Cantt, Pakistan, in 1979. He received his B.S. degree with honors in Electrical Engineering from the University of Engineering and Technology, Lahore, Pakistan in 2002. He obtained his M.S. degree in Microwaves and Optoelectronics from ENSEEIHT, Toulouse, France in 2006.

He is currently working toward the Ph.D degree in optronics and microwaves at the "Institut Supérieur de l'Aéronautique et de l'Espace" (ISAE), Toulouse, France. His research interests include optical

injection-locking and high-speed modulation of VCSELs, generation of high spectral purity microwave signals, optical communication systems and opto-microwave applications for embedded systems.



**Alexandre Bacou** (M'07) was born in Moissac, France, in 1980. He received the M.S. degree in microwaves and opto-electronics in 2005 and the Ph.D. degree in microwave photonics in 2008 from the Institut Supérieur de l'Aéronautique et de l'Espace (ISAE).

Since 2009, he is doing a post-doctoral research on DWDM applications using long-wavelength VCSELs at ISAE. His research interests are in microwave photonics and include characterization and modeling of long-wavelength VCSELs, injection locking, and

optical communication systems.



**Angelique Rissons** was born in Reims, France, in 1975. She obtained the M.S degree in Microwave and Optoelectronics in 2000 and the PhD degree in 2003 from the "Grande Ecole" Supaéro (National School of Aeronautics and Space),Toulouse, France. Her thesis work was on the optoelectronic modelling and characterisation of 850nm VCSELs.

Since 2004, she has been with the MOSE (microwave and optoelectronics for embedded systems) research group. She is in charge of the VCSELs activities of DEOS (Department of "Electronics-Optronics-Signals" ) at the "Institut Supérieur de l'Aéronautique et de l'Espace" (ISAE).She is currently working on modelling and characterisation of longwavelength VCSELs in optical subassembly. She is also interested by the various applications of the VCSEL in avionic and optical access networks.



**Jean-Claude Mollier** received his Doctorate degree in 1982 from the University of Franche-Comté, Besançon,France. He worked first on stable RF oscillators at the Laboratoire de Physique et Metrologie des Oscillateurs until he joined,in 1984,the Research Institute in Optical and Microwave Communications (X-LIM, France) where he became manager of a research group in the field of broadband and low noise microwave amplification. Since 1991,he has been working about microwave-photonics interactions at SUPAERO-ONERA in Toulouse (France).

His research interests include optical generation of microwave signals, modeling and characterization of semiconductor Lasers (VCSELs and QCLs) for application in optical fiber links and THz active imaging.

He is currently Head of the Department "Electronics-Optronics- Signal" at the Institut Supérieur de l'Aéronautique et de l'Espace ( ISAE). Dr. J.-C.Mollier is a member of IEEE-LEOS and French Optical Society (SFO) where he founded the club "Optics and Microwaves" in 1995.

**Vladimir Iakovlev** Photo and biography not available at the time of publication.

**Alexei Sirbu** Photo and biography not available at the time of publication.

**Eli Kapon** Photo and biography not available at the time of publication.